J Supercond Nov Magn (2013) 26:1865–1868
DOI 10.1007/s10948-012-2042-y

ORIGINAL PAPER

Hotspot Temperatures Reached in Current-Driven Superconducting Niobium Filaments

K. Harrabi

Received: 2 November 2012 / Accepted: 3 December 2012 / Published online: 9 January 2013

Abstract In a superconducting microbridge too narrow to support vortex motion, the current-induced resistance occurs non-uniformly at definite spots designated as Phase-Slip-Centres (PSC). Further, if the core of a PSC happens to heat above the critical temperature T_c, a PSC may evolve into a normal propagating zone, or hotspot. The PSC's time of nucleation and the HS minimum current I_h are determined, which allows deriving without ambiguity the rate of heat transfer to the substrate, the latter is compatible with a phonon blackbody radiation model at the Nb/R–sapphire interface. The computation of the HS temperature is then straightforward, while the PSC case is more involved. However, the PSC core temperature can be obtained through an independent determination of the inelastic quasi-particle diffusion length $\Lambda_{qp} \sim 2.8$ μm. The results of these computations are consistent with all the specific cases, PSCs and HSs, measured experimentally.

Keywords Superconductivity · Non-equilibrium · Phase slip centre

1 Introduction

Phase-slip centres appear in narrow superconducting filaments, where the superconductivity is locally destroyed in a zone of a few micrometres of length, leading to an oscillation of the order parameter at the Josephson frequency rate, in which the phase changes by quanta of 2π [1, 2]. These PSCs were reported first as steps in the resistance *vs* temperature $R(T)$ transition of tin whiskers [3], then observed as jumps in the I–V characteristic curves of whiskers [3], and of microstrips [4, 5]. Once considered as typical manifestations of one-dimensional (1-D) superconductivity, which implies transverse dimensions not exceeding the coherence length ξ, PSCs have since been generalized into phase-slip lines for wide strips [6], and they have been observed in a number of materials. We will be mainly concerned by the case of Nb strips [7] deposited on sapphire substrates.

In this work, the critical current I_c refers to the threshold for PSC nucleation, and the corresponding current density is written J_c. At low temperatures, the PSC naturally evolves [7] into an ordinary normal zone, or hot spot (HS), with an internal temperature larger than the critical temperature T_c. We define I_h, the related minimum current, whose Joule effect is sufficient to maintain a localized normal zone above T_c. On increasing the bath temperature T_b, the more abrupt decrease of I_c compared to that of I_h reverses the situation, and thus places $I_c(T_b)$ below $I_h(T_b)$. In this case, the high-T resistive response observed experimentally remains a PSC [5, 7]. The aim of this paper is to estimate the temperature of PSC and HS based on the contributions of the phonons and of the electrons.

2 Fabrication Process and Experimental Setup

The film labelled FK was dc-sputtered (2 nm per second) at room temperature on R-plane sapphire wafers, after thorough etching of both the niobium target and the substrate. Contact pads were made out of gold and had a 200 nm thickness. The connections to the measurement setup were performed using silver paste. Characteristics of the measured

K. Harrabi (✉)
Physics Department, King Fahd University of Petroleum and Minerals, 31261 Dhahran, Saudi Arabia
e-mail: harrabi@kfupm.edu.sa

K. Harrabi
Laboratoire Pierre Aigrain, ENS, 24 rue Lhomond, Paris 75231, France

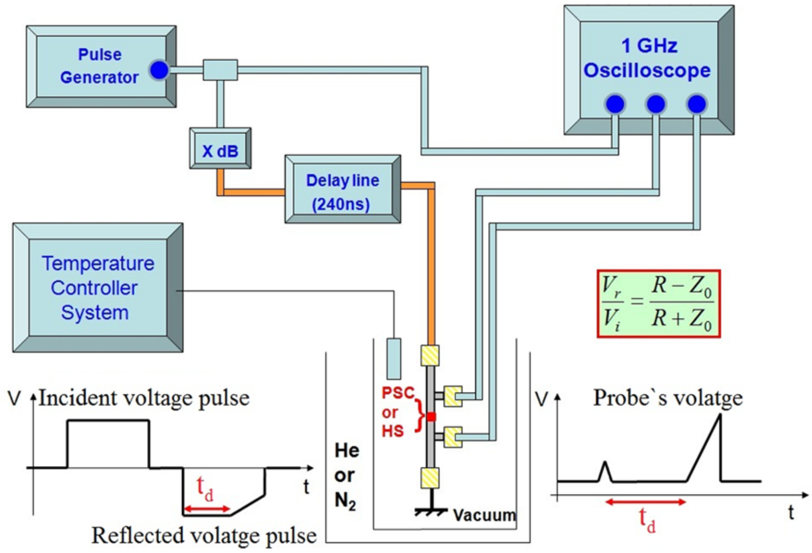

Fig. 1 Sketch of the experimental setup used for pulse measurements. It consists of a generator used to send a pulse, a delay line is needed to separate the incident pulse (V_i) from the reflected one (V_r), and an oscilloscope is used to measure the voltage and the delay time t_d. R represents the appeared resistance of the PSC or HS. The temperature controller is used to change the substrate temperature

sample are the thickness $b = 80$ nm, the width $w = 10$ µm, and the length $l = 3$ mm. The measurements at low current gave the critical temperature $T_c = 8.60$ K and the resistivity ρ (10 K) = 2.68 µΩ cm.

The sample is mounted in a ^{4}He cryostat and kept under vacuum. Our measurement consists of sending an electrical pulse of typically 400 ns at a repetition rate of 1 kHz, through 50 Ω coaxial cables and measuring the voltage response using lateral probes. A delay line of 240 ns was used to separate the incident voltage from the reflected one at the sample stage. Incident, reflected and lateral voltages were measured using a fast numerical oscilloscope. In this type of experiment, the voltage response to the pulse of current is a signal showing four features, starting with a positive inductive peak, followed by a zero voltage for a certain delay time t_d, then a voltage as a sign of the appearance of a resistive state and ending with a negative inductive peak. A schematic is shown in Fig. 1. The current reaching the sample in the superconducting state can be calculated, by considering that coaxial cables are lossless and the ohmic contacts are negligible. The current I through the strip is a function of the input voltage V_i, the instantaneous response voltage $V(t)$ measured by the lateral probe, and the line impedance Z_0. It is given by:

$$I = \frac{2V_i - V(t)}{Z_0}. \tag{1}$$

3 Discrimination Between Different Dissipative Modes

Sufficiently close to T_c, the first dissipative response occurs at the pair-breaking current $I_c(T)$. It corresponds to the nucleation of a PSC. The PSC response shows a quasi-stable voltage versus time (trace 1 in Figs. 3(a) and 3(b)). For $T \ll T_c$, the regime of flux flow is absent since the vortices

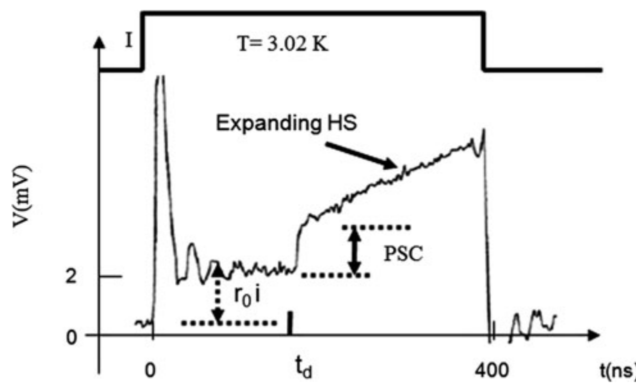

Fig. 2 Voltage response vs time of FK-91 at $T \ll T_c$ to a current pulse 400 ns of duration, it shows a PSC voltage step, a linearly rising HS voltage and r_0 is the contact resistance

are pinned. When the current is increased, a PSC is nucleated then transformed to a HS. In Fig. 2, the sudden rise at $t_d \approx 180$ ns is assigned to PSC nucleation, the following linear rise to HS growth. Short rise times necessary for this double observation are responsible for the large inductive spike and ringing.

The PSC is discriminated from the vortex flow mode by a delay time t_d. This parameter is described by time-dependent Ginzburg–Landau (TDGL) equation simplified to the zero-dimensional case and given by [9, 10]:

$$t_d(I/I_c) = \tau_d \int_0^1 \frac{2f^4 df}{\frac{4}{27}(\frac{I}{I_c})^2 - f^4 - f^6} \tag{2}$$

where the prefactor τ_d of the integral was interpreted as the gap relaxation time. It will instead be treated here as an adjustable parameter to fit the experimental delay times. The integral is temperature dependent through I_c. The phonon escape time is deduced from Eq. (2), $\tau_{esc} = 2$ ns, by measuring the t_d dependence on the applied current [7, 11].

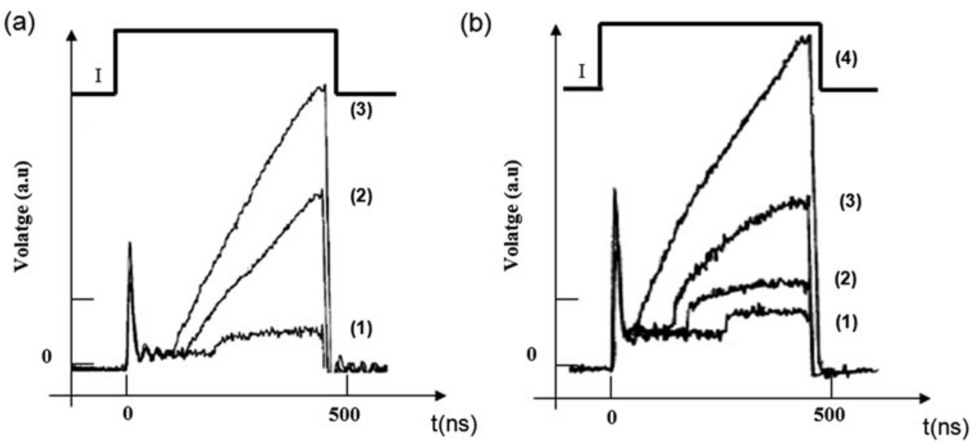

Fig. 3 (**a**) Time dependence of voltage across FK-91 bridge fed with current steps. Trace *1* (current 21.7 mA; 3.35 mV/vertical division): PSC signal (≈1.9 mV) nucleated at time $t_d = 220$ ns. Traces *2* (33.5 mA; 7.10 mV/div) and *3* (39.2 mA; 7.10 mV/div) display quasi-linearly increasing voltages, characteristic of hot spots. The initial inductive peak and following ringing are inessential features. (**b**) Time dependence of voltage across Nb bridge FK-91 for several conditions of temperature and current. Compare the flat PSC signal (1) (current 16.5 mA; 1.94 mV/vertical division, $T_b = 6.0$ K). Trace *2* (current 21.3 mA; 1.90 mV/vertical division, $T_b = 5.8$ K) as a PSC signal with strong heating. Trace *3* (current 25.2 mA; 2.15 mV/vertical division, $T_b = 5.2$ K) as an HS signal fed with a current slowly decreasing with the time. Vertical sensitivities in millivolts per division are: (i) 1.90; (ii) 1.94; (iii) 2.15 and (iv) 4.45

The other dissipative mode is the HS showing a linear increase of the voltage versus time compared to PSC, as shown in Figs. 3(a)—traces 2, 3 and 3(b)—traces 3, 4. Moreover, HSs and PSCs can be distinguished by a computation of their core temperature, above and below T_c respectively, as it will now be shown.

4 Calculation of the Hot Spot's Temperature

We define $J_u(T_b)$ to be the current density that would exactly maintain the temperature T_c in a uniformly heated film in contact with a substrate at (bath) temperature T_b, so that:

$$\rho J_u^2 = \frac{C}{\tau_{\mathrm{esc}}}(T_c - T_b). \tag{3}$$

Order-of-magnitude estimates justify the assumptions of uniformity of the temperature across the film thickness, and the negligible change of the substrate temperature from T_b during the excitations pulse. Because of the heat conduction across the healing boundaries, a larger current density $J_h(T_b) \sim \sqrt{2} J_u(T_b)$ is required [5] to sustain an isolated HS upon a substrate at temperature T_b. The dependence of any of the two currents densities J_u and J_h upon T_b is parabolic near T_c. However, far below T_c, where the linear heat transfer model is invalid, one can make use of the blackbody radiation power density $\sigma_\varphi(T^4 - T_b^4)$ per unit film area, where σ_φ is the Stefan constant appropriate to acoustic phonons, to represent the heat loss through the interface with the substrate. That law derives merely from (a) a phonon specific heat $C_\phi = \beta T^3$, with β constant in the Debye regime, and (b) a temperature independent phonon escape time τ_{esc}. Combining these two assumptions leads to $\sigma_\varphi = b\beta/4\tau_{\mathrm{esc}}$, which ensures a blackbody emission power tangentially consistent with Eq. (3) in the limit $T \longrightarrow T_b$. Note that σ_φ and the boundary resistance R_K satisfy the relationship $4\sigma_\varphi T^3 R_K = 1$. For the HS core, the temperature is estimated by using the following formula:

$$\frac{\rho I^2}{w^2 b^2} = \sigma_\varphi\left(T_M^4 - T_b^4\right) = \frac{\beta}{4\tau_{\mathrm{esc}}}\left(T_M^4 - T_b^4\right). \tag{4}$$

For the PSC case, one must account for the reduced dissipation rate $\rho I(I - I_s)$ [8], but also add the heat conducted along the bridge, as the diffusion of the excess electron energy $\int C_{\mathrm{es}}(T)\,dT$, expression in which the integration runs from T_b of the bath up to temperature T_m of the PSC centre. The inelastic diffusion length Λ, which measures the penetration of the electric field into the superconductor ($\Lambda = 2.8$ μm), suffices to compute the temperature in the vicinity of the PSC centre [12]:

$$\frac{VI}{w \times b \times 2\Lambda} = \frac{\rho I(I - I_s(T))}{w^2 b^2} = \frac{\beta(T_m^4 - T_b^4)}{4\tau_{\mathrm{esc}}} \tag{5}$$

where V is the PSC voltage. Then the problem arises to select a value for the excess superconducting current. Besides the standard choice $I_s = (1/2)I_c(T_b)$ giving T_{m1}, we also compute an upper bound on T_m with the second choice $I_s = 0$ giving T_{m2}. Table 1 reports the results obtained for T_m (PSC) and T_M (HS) with no further adjustment of the parameters. Where $\beta(\mathrm{Nb}) = 135$ μJ mol^{-1} K^{-4} = 12.3 J m^{-3} K^{-4}, deduced from a Debye temperature of 241 K [13]. For "unambiguous" Phase-Slip Centres (traces 1 of Figs. 3(a) and

Table 1 Estimation of the central PSC temperature T_m and HS temperature T_M in current-driven niobium bridge FK-91 for different values of the current and substrate temperatures T_b shown in Figs. 1, 2 and 3. Bold characters pertain to the most plausible state observed (PSC or HS). The start $*$ points to a transient PSC state. T_{m1} and T_{m2} are estimated respectively with $I_s = 1/2 I_c$ and $I_s = 0$. I_s represents the excess superconducting current

T_b (K)	I (mA)	I_c (mA)	I_h (mA)	T_{m1} (K)	T_{m2} (K)	T_M (K)	Trace No.
5.8	21.7	20	20	**7.4**	8.25	10.85	1 in Fig. 3(a)
4.2	33.5	32	22.8	8.25	9.65	**13.25**	2 in Fig. 3(a)
1.58	39.2	37.2	24.8	8.7	10.35	**14.3**	3 in Fig. 3(a)
6.0	16.5	16	19.5	**6.95**	7.6	9.65	1 in Fig. 3(b)
5.7	21.3	21	21	7.2	**8.20**	10.75	2 in Fig. 3(b)
5.20	25.2	25	22	7.45	**8.6**	11.6	3 in Fig. 3(b)
4.30	33.6	32	22.5	8.3	9.65	**13.3**	4 in Fig. 3(b)
3.02	35.4	35.2	23.2	**8.3***	9.85	**13.6**	Fig. 2

3(b)), both $T_m(I_s = I_c/2)$ and $T_m(I_s = 0)$ clearly fall below $T_c = 8.6$ K: the onset of HS formation is not reached. Well-growing HSs are recognisable in Fig. 2, in trace 3 of Fig. 3(a), or 1 of Fig. 3(b). In these cases, we note that $T_m(I_s = 0)$ passes well over T_c, which confirms that a PSC cannot survive the assigned values of bath temperature and current. Traces 2 and 3 of Fig. 3(b) are too complex to be described here. However, we note a clear discontinuity (jump from traces 3 to 4) on slightly increasing the current. Computations confirm that the PSC core temperature comes very close to T_c in these cases.

Let us recall that these evaluations were performed without any adjustable parameter. We also note that the compatibility between each box of Table 1 and the observed responses would be destroyed by a shift of only 1 K in T_m or T_M. Among all the parameters involved, τ_{esc} deserves a special mention since it derives, according to an original process [7], from the measured PSC nucleation times. This work may be considered as a test of significance and quantitative validity of that operation.

5 Conclusion

In conclusion, we have estimated the temperature of the PSC and HS, by taking into account the contribution of the phonon and the quasi-particles generated after the destruction of the superconductivity. Quantitatively, the assumption of a phonon blackbody radiation-law proves superior to a linear model of heat transfer. Let us note that our phonon escape times, common to both models, do not rely on quasi-static heat transfer measurements, but rather were inferred from the observed PSC nucleation times. In some conditions, vortex flow can coexist with the present localized modes, but the possible interference with the PSC nucleation is a problem still to be solved.

Acknowledgements K.H. gratefully acknowledges the support of the King Fahd University of Petroleum and Minerals, Saudi Arabia, under the IN100034 DSR project.

References

1. Tinkham, M.: Introduction to Superconductivity, 2nd edn. McGraw-Hill, Singapore (1996). Chap. 11
2. Rieger, T.J., Scalapino, D.J., Mercereau, J.E.: Phys. Rev. B **6**, 1734 (1972)
3. Webb, W.W., Warburton, R.J.: Phys. Rev. Lett. **20**, 461 (1968)
4. Meyer, J.D.: App. Phys. **2**, 303 (1973)
5. Skocpol, W.J., Beasley, M.R., Tinkham, M.: J. Low Temp. Phys. **16**, 145 (1974)
6. Sivakov, A.G., Glukhov, A.M., Omelyanchouk, A.N., Koval, Y., Müller, P., Ustinov, A.V.: Phys. Rev. Lett. **91**, 267001 (2003)
7. Ladan, F.-R., Harrabi, K., Rosticher, M., Mathieu, P., Maneval, J.-P., Villard, C.: J. Low Temp. Phys. **153**, 103 (2008)
8. Skocpol, W.J., Beasley, M.R., Tinkham, M.: J. Appl. Phys. **45**, 4054 (1974)
9. Pals, J.A., Wolter, J.: Phys. Lett. A **70**, 150 (1979)
10. Tinkham, M.: In: Gray, K.E. (ed.) Non-Equilibrium Superconductivity, Phonons and Kapitza Boundaries, Chap. 8, NATO Conference. Plenum, New York (1981)
11. Harrabi, K., Cheenne, N., Boyer, F., Chibane, F., Delord, P., Ladan, F.-R., Maneval, J.-P.: Supercond. Sci. Technol. **13**, 1222 (2000)
12. Kadin, A.M., Skocpol, W.J., Tinkham, M.: J. Low Temp. Phys. **33**, 481 (1978)
13. Leupold, H.A., Boorse, H.A.: Phys. Rev. A **134**, 1322 (1964)